Measurement of the tZq Differential Cross-section with the ATLAS Detector at the LHC

Dissertation
zur
Erlangung des Doktorgrades (Dr. rer. nat.)
der
Mathematisch-Naturwissenschaftlichen Fakultät
der
Rheinischen Friedrich-Wilhelms-Universität Bonn

vorgelegt von
Nilima Akolkar
aus
Vadodara, India

Bonn 2024

Angefertigt mit Genehmigung der Mathematisch-Naturwissenschaftlichen Fakultät der Rheinischen Friedrich-Wilhelms-Universität Bonn

1. Gutachter: Prof. Dr. John Smith
2. Gutachterin: Prof. Dr. Anne Jones

Tag der Promotion:
Erscheinungsjahr:

Contents

Todo list

CHAPTER 1

Theoretical Concepts and Experimental Basics

1.1 The Standard Model (SM)

In the 19th century, John Dalton postulated that matter is made up of small indivisible pieces called atoms. Since then, technological advancements and human curiosity have empowered us to explore various phenomena around us in greater detail. Eventually, our understanding of nature evolved, leading to the development of the Standard Model of Particle Physics, which explains the fundamental structure of matter. Consisely speaking, the Standard Model (SM) of particle physics is a theory that explains almost everything that nature has to offer. It is based on fundamental particles and their interactions being governed by Quantum Field Theories (QFTs). The SM has precisely predicted existence of various particles and their properties. Testing the SM and its predictions plays a crucial role in deciding the physics program of Particle Physics experiments.

The Standard Model is divided into spin-1 fermions and spin-0 bosons. The fermions are further divided into leptons and quarks as shown in Fig. 1.1. Another classification of fermions is into generations. The first generation constitutes u, d, e^- and ν_e which forms the surrounding matter. The second and third generation particles are high energy *siblings* of the first generation particles. These are observed at high energies such as colliders. The SM also includes anti-particles which are clones of particles with opposite quantum numbers.

These fermions interact with each other via exchanging bosons which are also called *force-carrier* particles. The photon (γ), which is massless and carries no electric charge, is the messenger of the electromagnetic (EM) force, experienced only by charged particles. The underlying QFT is called Quantum Electrodynamices (QED) based on the U(1) symmetry group. The more commonly known electrostatic attraction between charged particles is the low-energy manifestation of QED. Among the SM, all fermions except neutrinos are sensitive to the EM force. The strength of the EM force is expressed by its dimensionless coupling constant,

$$\alpha \sim \frac{1}{137} \tag{1.1}$$

The strong interaction, mediated by massless gluons, is experienced by particles carrying the so-called *colour* charge. The physics behind the strong interaction is explained in Quantum Chromodynamics (QCD). The quarks, which are the only particles carrying colour charge, can interact via the strong interaction. A peculiar thing in QCD is that the gluons themselves also carry colour charge. This

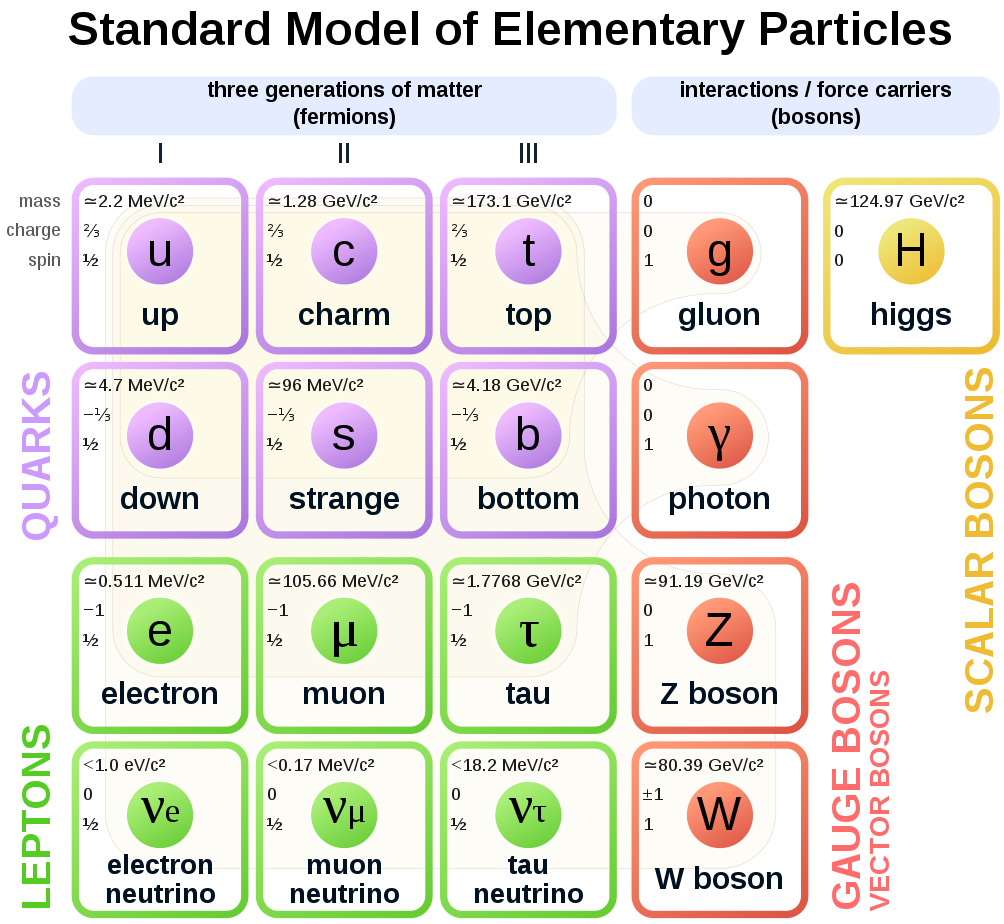

Figure 1.1: Overview of the particles in the Standard Model along with their properties including mass, spin and charge are shown. Particles shown in lavender and green are fermions while the ones shown in red are gauge bosons. The three generations are also highlighted by roman letters. Anti-particles are not shown [1].

property is unique for a force-carrier particle.

The weak force carriers are the vector bosons, $W^{\pm}$ and Z, which unlike γ and gluons, are massive and charged in case of $W^{\pm}$ boson. The Z boson is electrically neutral. The weak interaction manifests itself in phenomena such as β-decay and fusion processes inside the sun. All the SM particles, including the neutrinos, are sensitive to the weak force. The interaction mediated by $W^{\pm}$ and Z is called charged-current weak interaction and neutral-current weak interaction, respectively. The famous Wu experiment [2] proved that the charged current weak interaction violates parity. The parity violating nature of the weak interaction suggests that the interaction vertex must be different from that of QED and QCD. Studies showed that the weak interaction is described using a $V - A$ vertex and this fact dictates that only left-handed chiral particle states and right-handed chiral antiparticle states can participate in charged-current weak interaction.

The theory unifying QED and the weak interaction is called the Electroweak theory explained in Section 1.1.3. The last piece of the SM puzzle, which is the last discovered fundamental particle, is the Higgs boson. It is a spin-0 boson, unlike other bosons. All particles acquire their mass through the Higgs mechanism.

1.1.1 Feynman diagrams

There are numerous probable interactions between SM particles and having a tool to visualise them would greatly aid in understanding the underlying physics. In Particle Physics, a tool called Feynman diagrams is used for this purpose.

These diagrams are symbolic representations of particle interactions. They make use of straight lines with arrows to show incoming and outgoing particles and anti-particles. Wavy lines are used to show the boson exchanged between them. It also has a hypothetical time axis which demonstrates the evolution of the process with time. The Feynman diagrams are just a pictorial representation and have no physical meaning.

Consider an example of electron-position scattering (also known as Bhabha scattering). In the Feynman diagram, shown in Fig. 1.2, let's suppose a horizontal time axis. The diagram reads as following: an electron and positron enter, a photon is exchanged between them and the two particles exit. The point of interaction between two particles is called a *vertex*. It is important to note the direction of arrows in particle lines. The arrow directions are opposite for particles and antiparticles. In the shown diagram, the incoming electron points in the forward direction, denoting the evolution of the interaction with time, whereas the incoming positron points in the backward direction. It can be seen that the arrow directions together represent the continuous current flow.

The quantitative analysis for a process includes two important steps: accessing the Feynman diagrams to compute the amplitude ($\mathcal{M}$) and together with the phase space, calculating quantities such as decay rate, cross-section and differential cross-section. The Feynman diagrams are analysed through a set of rules called Feynman rules. It is important to note that for each process, there are infinite possible Feynman diagrams which require to be summed to get the accurate final process description. The diagram shown in Fig. 1.2 is a basic diagram with particles entering and exiting, called real particles with specific masses. A process can also have intermediate stages where off-shell intermediate particles with varying masses, called *virtual* particles are produced. Presence of intermediate states lead to more vertices inside a diagram and therefore give rise to a plethora of Feynman diagrams for a certain process.

In the context of Feynman calculus, each vertex within a diagram contributes a factor equal to

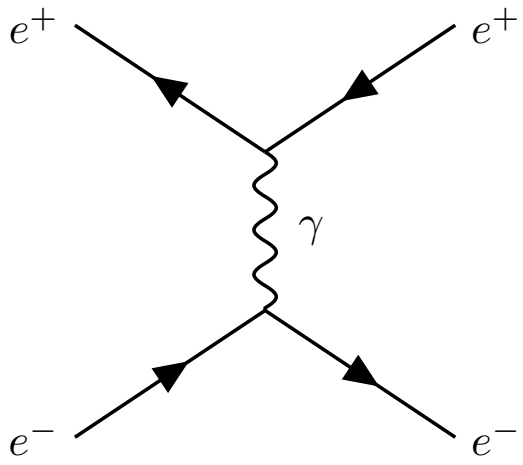

Figure 1.2: A Feynman diagram showing the Bhabha scattering

the coupling constant of the interaction. Hence, the actual process can be quantitatively described in terms of expansion with respect to the coupling constant. For the expansion to converge, the coupling constant needs to be small. The most basic diagram with the lowest order expansion is called "tree-level" or "leading-order (LO)" diagram. The diagram corresponding to the next order of expansion is called next-to-leading-order (NLO). Higher order diagrams with more vertices contribute less owing to the small couping constant.

1.1.2 The Strong Force

Electrons and nucleus inside an atom are held together by the electromagnetic force. The same force also exists between protons inside the nucleus causing repulsion. However, there exists a force which is strong enough to overcome repulsion and keep the nucleus together. It is called the strong force or the strong nuclear force. The QFT describing the strong force is called Quantum Chromodynamics (QCD) and the underlying symmetry group is SU(3) described by 3×3 matrices. The eight generators of the SU(3) group give rise to eight gluons which are the strong force mediators. The structure of the SU(3) group demands that the wave function of the strongly interacting particle must be a 3-component vector. This gives rise to a new degree of freedom called "colour", with three states called red, blue and green. Consequently, particles having a non-zero colour charge can feel the strong force. Among the SM particles, only quarks have the colour charge which can be either red, blue or green.

A major differentiating factor between QCD and QED is that the gauge boson in QCD carries the charge of interaction. In other words, gluons also carry the colour charge which allows them to interact with other gluons as well. As a result of this self-interaction, no coloured object can be found as a free particle in nature. Due to this so-called colour confinement, quarks cannot exist independently but instead are found in colour-neutral states called *hadrons*. For instance, if two quarks are pulled away from each other, a gluon field is created between them which is proportional to the separation. The gluon fields is so strong that at some point, the energy in this field is sufficient to produce new quarks and antiquarks that form colourless bound states. This process is called hadronisation. Due to colour confinement, only certain configurations for hadrons are permitted. The possible combinations discovered so far can be categorised into mesons ($q\,\overline{q}$), baryons ($q\,q\,q$) and antibaryons ($\overline{q}\,\overline{q}\,\overline{q}$).

The value of the strong coupling constant, α_S, is relatively larger than the coupling constant of QED. As a consequence, contribution of higher order Feynman diagrams increases and it becomes difficult to implement perturbation theory for QCD calculations. One of the great discoveries in QCD is that the strong coupling constant is in fact not a "constant" but instead the value is dependent on the energy scale of the interaction [3]. The running of α_S means that at low energies, the force between the quarks is stronger (larger α_S) whereas at higher energies, the force becomes weak (smaller α_S). The running of α_S allows us to apply perturbation theory at high energies and this property is called asymptotic freedom.

1.1.3 The Electroweak theory

In the 1960s, physicists were trying to formulate a gauge theory for weak interactions similar to QED. A theory can be a gauge theory if it has an underlying mathematical symmetry and it is renormalisable. A quantum field theory is renormalisable if the divergences can be absorbed by implementing finite number of parameters, such as, coupling constant. Glashow, Salam and Weinberg discovered such a gauge theory by unifying electromagnetic force and the weak force.

The electroweak (EW) theory is a unification of QED and the thoery of weak interactions. It is described by the symmetry group $SU(2)_L \otimes U(1)_Y$. The corresponding charges of the electroweak theory are the weak isospin I, I_3 and the weak hypercharge Y. The weak hypercharge Y determines the interaction under the $U(1)$ transformations. The weak isospin of particles determines their transformation under $SU(2)$ and therefore, it is used to make multiplets of particles. The left-handed leptons (ℓ_L) will form doublets because they transform into each other under the influence of weak force. This is due to the $V-A$ vertex form of the weak interaction. On the other hand, the right-handed particles are singlets (ℓ_R).

$$\ell_R = e_R^-, \mu_R^-, \tau_R^- \tag{1.2}$$

$$\ell_L = \begin{pmatrix} \nu_e \\ e^- \end{pmatrix}_L, \begin{pmatrix} \nu_\mu \\ \mu^- \end{pmatrix}_L, \begin{pmatrix} \nu_\tau \\ \tau \end{pmatrix}_L \tag{1.3}$$

The Lagrangian of the EW model introduces three bosons $W_\mu^{(1,2,3)}$ corresponding to $SU(2)$ and one B_μ corresponding to $U(1)$. Th experimentally observed $W^\pm$ are combination of $W_\mu^{(1)}$ and $W_\mu^{(2)}$ whereas photon (A) and the Z-boson are linear combinations of $W_\mu^{(3)}$ and B_μ based on the weak mixing angle (θ_W) as given below:

$$A_\mu = +B_\mu \cos\theta_W + W_\mu^{(3)} \sin\theta_W \tag{1.4}$$

$$Z_\mu = -B_\mu \sin\theta_W + W_\mu^{(3)} \cos\theta_W \tag{1.5}$$

The weak interaction for the quark sector can be explained by creating similar $SU(2)$ doublets(Q).

$$Q = \begin{pmatrix} u \\ d' \end{pmatrix}, \begin{pmatrix} c \\ s' \end{pmatrix}, \begin{pmatrix} t \\ b' \end{pmatrix} \tag{1.6}$$

The strength of the weak interactions for quarks is determined experimentally by studying nuclear β-decay. It is observed that the vertices corresponding to different quark flavours have different coupling strengths. The reason for this is given by the Cabibo hypothesis which states that, the flavour eigen states that participate in the weak interactions are a mixture of the mass eigen states. The relation between them is given by the Cabibo-Kobayashi-Maskawa (CKM) matrix.

$$\begin{pmatrix} d' \\ s' \\ b' \end{pmatrix} = \begin{pmatrix} V_{ud} & V_{us} & V_{ub} \\ V_{cd} & V_{cs} & V_{cb} \\ V_{td} & V_{ts} & V_{tb} \end{pmatrix} \begin{pmatrix} d \\ s \\ b \end{pmatrix} \tag{1.7}$$

The values of the CKM matrix elements can be found in [4]. The diagonal of the matrix is close to unity, suggesting that the weak interaction is stronger within the same generation of quarks.

The experiments at the Gargamelle bubble chamber in 1973 hinted the evidence of a neutral massive boson responsible for the observed neutrino interactions [5]. In 1983, the Z-boson was directly discovered at the Super-Proton Synchrotron at CERN. The electroweak theory was verified by this pathbreaking discovery. The properties of the Z-boson were studied at the Large Electron-Positron (LEP) collider at CERN. The discovery of Z and W bosons are among the crucial tests of the Standard Model.

1.1.4 The Higgs mechanism

According to the electroweak theory, weak bosons are required to be massless for the underlying symmetry to be preserved. However, experiments revealed that the weak gauge bosons, W and Z have finite masses [6]. The explanation of this spontaneous symmetry breaking was given by the Brout-Englert-Higgs mechanism [7]. Particles in the SM acquire their mass through the Higgs mechanism. It is a way of spontaneously breaking SM symmetries by introducing a new field called the Higgs field. The strength of interaction of particles with this field determines how massive the particles will be. Higgs mechanism implies the existence of a scalar particle, the SM Higgs boson. In a landmark discovery, the Higgs boson was independently discovered by ATLAS and CMS in 2012 [8, 9]. Since then, the Higgs boson studies are an important part of the LHC physics program.

1.2 Limitations of the SM

The Standard Model is a highly successful theory that has been tested at various collider experiments and almost all the experimental results agree with the predictions, at a high degree of precision. Despite its enormous success, there are still some drawbacks of the SM. They are summarised below:

- Out of the four fundamental forces, only three are explained in the SM. Gravity is not included.
- SM predicts that neutrinos are massless but experiments have proved that neutrinos are not massless.
- The difference in the mass scale of vector bosons/Higgs boson and the Plank scale is extremely large. This is known as the hierarchy problem and is unexplained by the SM.
- There is no explanation of why is there more matter around us than antimatter.

- The possible existence of dark energy and dark matter is hinted from studies regarding expansion of the universe. There is no explanation in the SM.

1.3 Physics at the hadron colliders

Center-of-mass energy

In a collision between two particles the total center-of-mass energy is expressed as

$$\sqrt{s} = \sqrt{(\Sigma_{i=1}^{2} E_i)^2 - (\Sigma_{i=1}^{2} p_i)^2}, \tag{1.8}$$

where E and p are energy and momentum of the two initial state particles. If two colliding beams of the same particle type have the same energy, then the center-of-mass energy is $\sqrt{s} = 2E_{beam}$, neglecting the masses of particles.

Decay rate and branching ratio

An elementary particle often decays into smaller particles through the possible decay modes or channels, depending on the conservation laws for quantum numbers and strength of the decay process. The probability per unit time of a particle decaying is called its decay rate (Γ). For N identical particles the change in the number after time dt is given by

$$dN = -\Gamma N dt. \tag{1.9}$$

The lifetime of the particle is the time after which the sample becomes $\frac{1}{e}$ of its original size,

$$\tau = \frac{1}{\Gamma}. \tag{1.10}$$

When multiple decay modes are possible, the total decay rate of the particle is the sum of individual decay rates. In order to learn the dominance of a certain decay mode, we calculate its branching ratio (BR). The branching ratio of a decay mode i is defined as

$$\mathrm{BR} = \frac{\Gamma_i}{\Gamma_{\mathrm{total}}}. \tag{1.11}$$

Parton Distribution Functions (PDFs)

Protons at the LHC collide at high energies giving rise to deep inelastic interactions called hard processes. In such cases, the interactions are not between protons but between their constituents which are quarks and gluons, collectively known as *partons*. These partons carry a fraction of the total momentum of the proton (or a hadron in general). In order to study an interaction, it is important to know the effective energy of the interacting partons and their flavour. This information is encoded in the Parton Distribution Functions (PDFs). It provides quantitative information regarding the distribution of energy carried by the quarks and gluons inside a proton. A PDF describes the probability of finding a parton of certain flavour i, carrying a momentum fraction x_i at a certain energy scale. The PDFs are extracted from experimental data.

Pileup

The primary hard scatter collisions, that are of interest, are contaminated by soft interactions called pileup. It is defined by the average number of interactions recorded per bunch crossing. Sources of pileup are categorized into in-time and out-of-time pileup. In-time pile up is due to collisions occurring in the same bunch-crossing and out-of-time pile-up is contributed by the collisions from previous or later bunches. Some of the sub-detectors have sensitivity windows longer than the interval between bunch crossings. This eventually affects the recorded number of interactions per bunch. The accurate detection of objects under study becomes difficult due to pile-up events. The higher the luminosity, more the pileup. The object reconstruction algorithms have dedicated procedures to mitigate pileup.

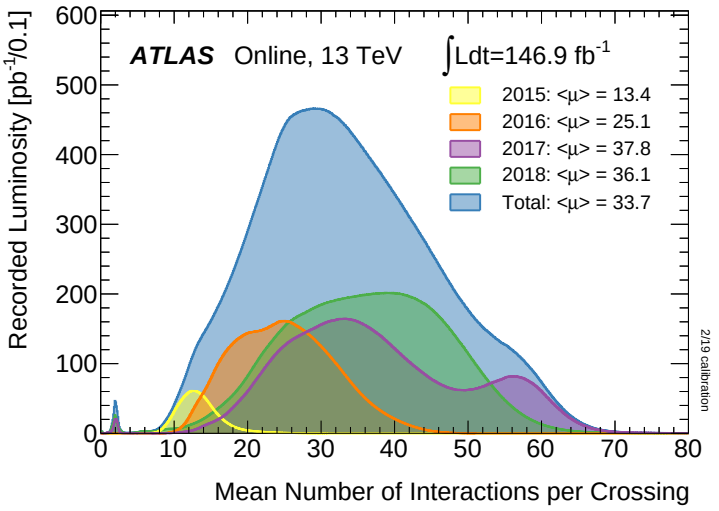

Figure 1.3: [10].

Luminosity and cross-section (σ)

The quantity that measures the ability of a collider to produce particle interactions is called instantaneous luminosity ($\mathcal{L}$). The instantaneous luminosity integrated over the lifetime of collider operation is called integrated luminosity (L). During the operation of the LHC from 2015 to 2018, the delivered integrated luminosity is shown in Fig. 1.4.

In order to define the event rate for interesting processes, along with luminosity, we require another quantity called the cross-section. At the subatomic scale, the particle interactions are governed by the laws of quantum physics. Therefore, a theory can predict the *probablility* of certain outcomes of collisions. The probability of a certain process to occur is called its cross-section (σ). Finally, the number of event rate of specific interactions is defined as the product of integrated luminosity and the cross-section (Eq. (1.12)).

$$R = \sigma \cdot \int_{dt} \mathcal{L}(t) \tag{1.12}$$

For a particle collider, beam energies and the luminosity are two important figures of merit. High

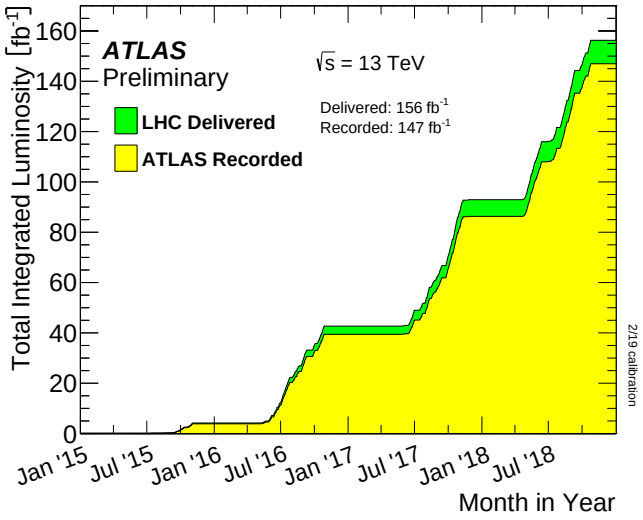

Figure 1.4: [11].

energy allows the production of new heavy particles and high luminosity allows more flux of particles contributing to high number of collisions.

Differential cross-section

Differential cross-section is a type of cross-section which gives the probability of an interaction with respect to a variable X. In common practice, differential cross-section is defined as $d\sigma/dX$, where dX can be solid angle in scattering experiments or kinematic variables such as p_{T}. The integral over the entire range of X gives the total cross-section.

The differential cross-section offers a deeper insight into the process of interest. For example, in a scattering experiment designed to investigate the internal structure of a target, the scattering profile of the incident particles is analysed. If the scattering rate varies at different solid angles, this variation will be captured in the differential cross-section measurements.

Another advantage of studying differential cross-section is that if there is any new physics, it may manifest itself by altering the kinematic distributions of known SM particles. Measuring the differential cross-sections with respect to kinematic variables and then comparing them to SM predictions is one of the crucial tests of the SM. Any deviations in the comparison can hint towards new physics. A differential analysis is based on the shape of the kinematic distribution and not just the total events in the distribution. Therefore, differential cross-sections can be used for various theory interpretations.

1.4 Top quark physics

The electroweak theory states that the left-handed particles forming weak isospin doublets can interact weakly. In 1977 the bottom quark was discovered and it led to the prediction of its weak isospin partner, the top quark t. This prediction was made to keep the electroweak theory internally consistent. After puzzling the scientists for around two decades, the first observation of the top quark was in 1995

at the Tevatron collider at Fermilab by CDF and D0 collaborations [12, 13]. The top quark is the heaviest fundamental particle discovered so far with a mass of (172.57 ± 0.29) GeV [14].

The top quark being the weak isospin partner of the bottom quark, completes the three generation structure of the SM. Since its discovery, the top quark has been a crucial part of the physics programs at hadron colliders because of its unique properties. The lifetime of the top quark is so short that it decays before it can hadronise. This property gives us a unique opportunity to study a "bare" quark because some of its properties are conserved in the decay process and passed on to its decay products. Regarding the decay products, the top quark decays almost exclusively into a W boson and a b quark.

Study of the top quark is interesting due to various reasons. Its large mass suggests strong coupling to the Higgs field, therefore studying top quarks can give insights into the Higgs sector. In addition, evidence of new physics can be possibly extracted from top quarks because several beyond SM physics models suggest that heavy particles might decay into top quarks [15].

After the shutdown of the Tevatron, LHC remains the only place to produce top quarks in abundance, which is why the LHC is called a top factory. Due to the large center of mass energy, processes involving top quarks along with heavy bosons are also possible at the LHC. These processes are sensitive to electroweak and strong couplings. Therefore, precise measurements in this field can prove as an important test of the SM.

1.4.1 Production modes

The top quark can be produced either as a top-antitop pair in the so-called pair production mode or as a single top in association with a light quark or a W-boson. The most dominant mode is the pair production mode mediated by the strong force. The single top production proceeds via the electroweak interaction as discussed below. Studying the different production channels of the t-quark offers insights into QCD and the electroweak sector. Moreover, measurements of the cross-sections are used to extract important parameters of the SM such as the top quark mass.

Pair production

At LHC energies, gluons inside protons are prone to numerous self interactions and splitting which in turn produces more and more gluons available for production of heavy particles. The dominant production of top quarks at the LHC is the top-antitop ($t\bar{t}$) pair production [16]. It is initiated either by gluon-gluon fusion, which is the dominant channel, or through quark-antiquark annihilation. The leading-order Feynman diagrams are shown in Fig. 1.5. The inclusive cross-section of the $t\bar{t}$ production measured by ATLAS and CMS collaborations at $\sqrt{s}$=13 TeV is shown in Fig. 1.6. The results are found to be in agreement with the SM prediction. The measurements of top pair production is useful for studying PDFs, specifically gluon PDFs [17].

Single-top production

There are three separate processes at LO leading to the production of a single-top quark. Based on the virtuality of the exchanged W-boson, the possible modes are t-channel, s-channel and associated Wt-channel as shown in Fig. 1.7. The t-channel process is initiated by a b-quark and a spectator quark, producing a single top and a light jet. This process has the largest production cross-section at the LHC. The s-channel is characterised by a quark-antiquark pair interacting to produce a single

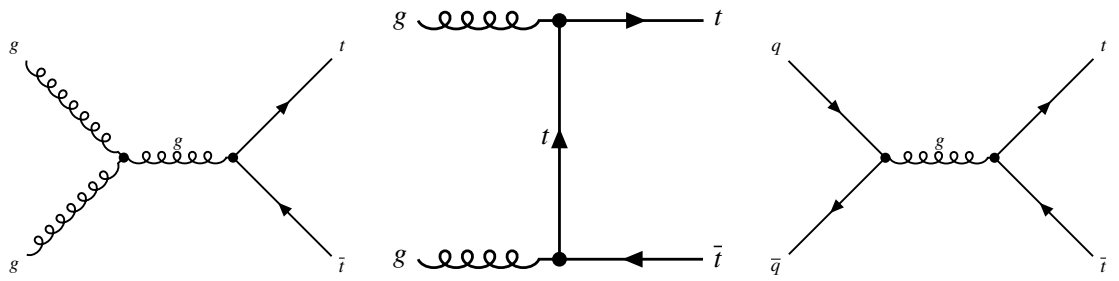

Figure 1.5: Feynman diagrams for $t\bar{t}$ processes at LO in QCD. The gluon-gluon fusion process which is the dominant mode is shown in the leftmost diagram.

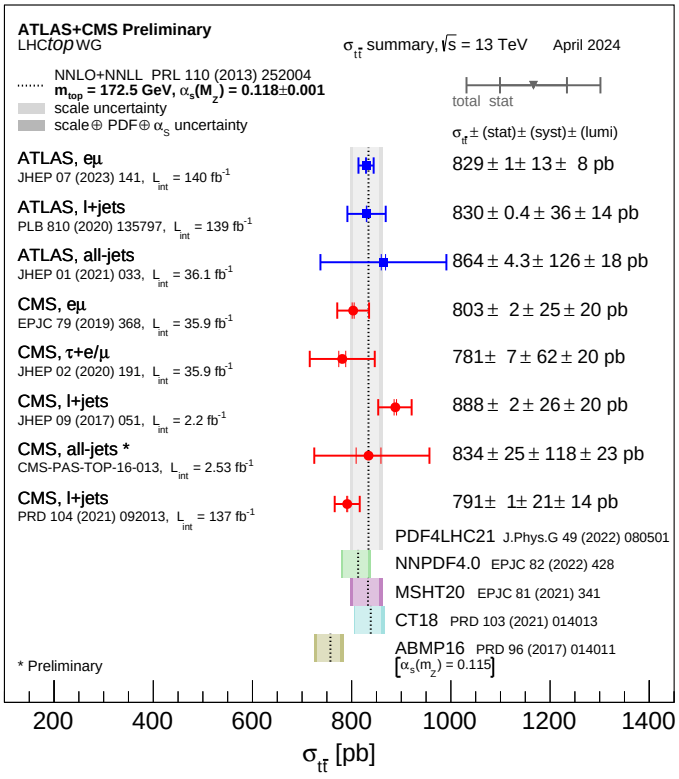

Figure 1.6: Summary of measurements of the $t\bar{t}$ production cross-sections in different analysis channels by ATLAS and CMS at $\sqrt{s}$=13 GeV. The results are compared with NNLO QCD predictions [18].

top and a bottom quark. The requirement of an antiquark in the initial state largely suppresses this process [19]. In the associated Wt-channel, a gluon and a bottom quark produces a single top and an on-shell W-boson. Its final state is same as the $t\bar{t}$ process with one less b-jet. The associated Wt process is an important background for other top quark and Higgs related measurements [20].

Due to the electroweak nature of the single top production, it is sensitive to various parameters such as the V_{tb} element of the CKM matrix and the Wtb coupling [21]. The single top production cross-section measurements by ATLAS and CMS are shown in Fig. 1.8.

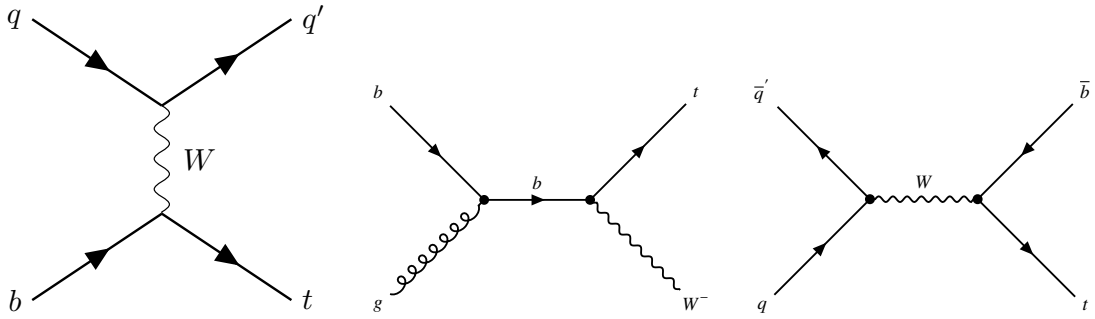

Figure 1.7: Feynman diagrams for single top production processes at LO in QCD. The possible production modes namely t-channel (left), associated Wt-channel (middle) and s-channel (right) are shown. The largest cross-section is of the t-channel, followed by the Wt-channel. The s-channel is highly suppressed.

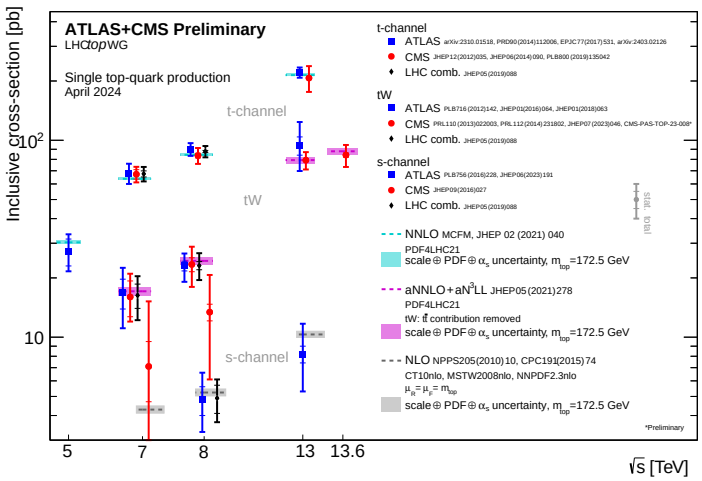

Figure 1.8: Summary plot showing inclusive cross-sections of the single-top production modes measured at different center-of-mass energies by ATLAS and CMS [18].

1.4.2 Rare associated top quark processes

Measurements of rare processes at the LHC are important tests to validate the SM. Therefore, physics program at the LHC is heavily involved in precision measurements related to rare processes, especially those involving top quarks. The top quark being the heaviest fundamental particle so far, has strong

links to the Higgs sector and also to potential BSM physics. Moreover, top quark associated processes probe electroweak couplings of the top quark which are fundamental parameters of the SM. Therefore, it is relevant to study rare processes involving top quarks. The production cross-sections of various top quark associated processes are shown in Fig. 1.9.

The associated production of a single top with a photon, called $tq\gamma$ production, probes the coupling between top and photon. It is studied using the full 13 TeV dataset by ATLAS and CMS in the leptonic channel due to the higher sensitivity compared to hadronic channels. The measured cross-section is in agreement with the SM prediction [22].

The evidence for an associated production of a top quark with two heavy bosons (tWZ) is reported by the CMS collaboration. Studies are performed using the 13 TeV dataset in the leptonic channel and the measured cross-section corresponds to a statistical significance of 3.4 standard deviations [23].

The associated process of a top quark and a Z boson, called the tZq production, is one of the rare processes at the LHC and it is the main focus of this thesis. This process is interesting because it probes two different kinds of couplings through the same interaction. Detailed description is given in **??**.The cross-sections of tZq, tWZ and $tq\gamma$, as measured by ATLAS and CMS, are compared in Fig. 1.10. The tZq process is also useful in studying Flavour-Changing-Neutral-Current (FCNC) couplings. The SM forbids interactions of fermions with Z boson, where the flavour of the incoming quark is changed. However, some extension models of SM predict otherwise. A dedicated search for FCNC processes involving a top quark, an up-type quark and Z boson was conducted by ATLAS using the full Run-2 dataset. The goal was to look for events corresponding to either ($gq \rightarrow tZ$) or events where t decayed into Z ($t \rightarrow qZ$). Despite the efforts, no evidence for FCNC processes was found [24].

One of the rarest and heaviest process at the LHC is the production of four tops ($t\bar{t}t\bar{t}$). This process is interesting because it simultaneously probes the coupling of four fermions. In addition, various BSM models predict potential modification in the cross-section, hinting towards new physics. The four tops production was observed at the LHC at 6.1 standard deviation and its cross-section, measured by the ATLAS experiment using 140.1 fb^{-1}at 13 TeV center-of-mass energy, is ($22.5\,^{+6.6}_{+5.5}$) fb [25]. It is found to be consistent with the SM prediction.

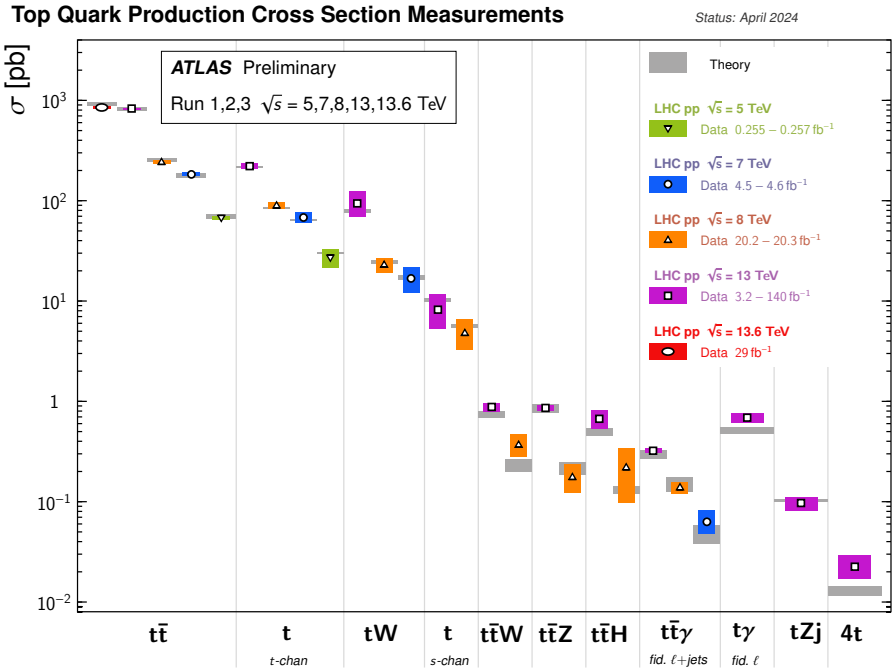

Figure 1.9: Different processes involving top quarks are shown in decreasing order of their cross-sections. A clear difference in the cross-section is visible in the dominant $t\bar{t}$ process and the rarest four tops process. The tZq process falls towards the tail of the plot implying that it is one of the rare processes [18].

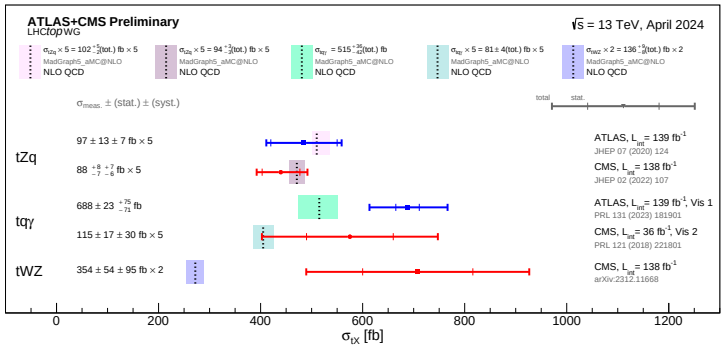

Figure 1.10: Production cross-sections of single top quark associated processes measured by ATLAS and CMS experiments [26].

Bibliography

[1] *Standard Model of Particle Physics*, Accessed on: 30.09.2024, URL: https://en.wikipedia.org/wiki/Standard_Model (cit. on p. 2).

[2] C. S. Wu, E. Ambler, R. W. Hayward, D. D. Hoppes and R. P. Hudson, *Experimental Test of Parity Conservation in β Decay*, Phys. Rev. **105** (1957) 1413 (cit. on p. 3).

[3] A. Deur, S. J. Brodsky and G. F. de Teramond, *The QCD Running Coupling*, Nucl. Phys. **90** (2016) 1, arXiv: 1604.08082 [hep-ph] (cit. on p. 5).

[4] S. N. et al. (Particle Data Group), Phys. Rev. D 110, 030001 (2024), URL: https://pdg.lbl.gov/2024/api/index.html (cit. on p. 6).

[5] F. Hasert et al., *Observation of neutrino-like interactions without muon or electron in the gargamelle neutrino experiment*, Physics Letters B **46** (1973) 138, ISSN: 0370-2693, URL: https://www.sciencedirect.com/science/article/pii/0370269373904991 (cit. on p. 6).

[6] *The origins of the Brout-Englert-Higgs mechanism*, (2014), URL: https://cds.cern.ch/record/1998492 (cit. on p. 6).

[7] P. W. Higgs, *Broken Symmetries and the Masses of Gauge Bosons*, Phys. Rev. Lett. **13** (16 1964) 508, URL: https://link.aps.org/doi/10.1103/PhysRevLett.13.508 (cit. on p. 6).

[8] G. Aad et al., *Observation of a new particle in the search for the Standard Model Higgs boson with the ATLAS detector at the LHC*, Phys. Lett. B **716** (2012) 1, arXiv: 1207.7214 [hep-ex] (cit. on p. 6).

[9] S. Chatrchyan et al., *Observation of a New Boson at a Mass of 125 GeV with the CMS Experiment at the LHC*, Phys. Lett. B **716** (2012) 30, arXiv: 1207.7235 [hep-ex] (cit. on p. 6).

[10] ATLAS Experiment, *Public Results*, 2024, URL: https://twiki.cern.ch/twiki/bin/view/AtlasPublic/LuminosityPublicResultsRun2#Annual_plots_on_the_Number_of_Pi (cit. on p. 8).

[11] ATLAS Experiment, *Public Results*, 2024, URL: https://twiki.cern.ch/twiki/bin/view/AtlasPublic/LuminosityPublicResultsRun2#Online_Luminosity_Summary_Plots (cit. on p. 9).

[12] F. Abe et al.,
Observation of Top Quark Production in $\overline{p}p$ Collisions with the Collider Detector at Fermilab,
Phys. Rev. Lett. **74** (14 1995) 2626,
URL: https://link.aps.org/doi/10.1103/PhysRevLett.74.2626 (cit. on p. 10).

[13] S. Abachi et al., *Observation of the Top Quark*, Phys. Rev. Lett. **74** (14 1995) 2632,
URL: https://link.aps.org/doi/10.1103/PhysRevLett.74.2632 (cit. on p. 10).

[14] S. Navas et al., *Review of particle physics*, Phys. Rev. D **110** (2024) 030001 (cit. on p. 10).

[15] M. Gallinaro, *Top quark physics: A tool for discoveries*,
Journal of Physics: Conference Series **447** (2013) 012012,
URL: https://dx.doi.org/10.1088/1742-6596/447/1/012012 (cit. on p. 10).

[16] M. Aaboud et al., *Measurement of the $t\bar{t}$ production cross-section using $e\mu$ events with b-tagged jets in pp collisions at $\sqrt{s}$=13 TeV with the ATLAS detector*,
Phys. Lett. B **761** (2016) 136, [Erratum: Phys.Lett.B 772, 879–879 (2017)],
arXiv: 1606.02699 [hep-ex] (cit. on p. 10).

[17] F. Fabbri, *Top pair production measurements at ATLAS*, Nuclear and Particle Physics Proceedings **282-284** (2017) 63, 19th International Conference in Quantum Chromodynamics,
ISSN: 2405-6014,
URL: https://www.sciencedirect.com/science/article/pii/S2405601416302607
(cit. on p. 10).

[18] *Top cross section summary plots - April 2024*, tech. rep., All figures including auxiliary figures are available at https://atlas.web.cern.ch/Atlas/GROUPS/PHYSICS/PUBNOTES/ATL-PHYS-PUB-2024-006: CERN, 2024, URL: https://cds.cern.ch/record/2896104
(cit. on pp. 11, 12, 14).

[19] M. Cristinziani and M. Mulders, *Top-quark physics at the Large Hadron Collider*,
Journal of Physics G: Nuclear and Particle Physics **44** (2017) 063001,
URL: https://dx.doi.org/10.1088/1361-6471/44/6/063001 (cit. on p. 12).

[20] G. Aad et al., *Measurement of single top-quark production in association with a W boson in pp collisions at $\sqrt{s}$ = 13 TeV with the ATLAS detector*, (2024), arXiv: 2407.15594 [hep-ex]
(cit. on p. 12).

[21] J. Andrea and N. Chanon, *Single-Top Quark Physics at the LHC: From Precision Measurements to Rare Processes and Top Quark Properties*, Universe **9** (2023) 439,
arXiv: 2307.14044 [hep-ex] (cit. on p. 12).

[22] G. Aad et al., *Observation of Single-Top-Quark Production in Association with a Photon Using the ATLAS Detector*, Phys. Rev. Lett. **131** (18 2023) 181901,
URL: https://link.aps.org/doi/10.1103/PhysRevLett.131.181901 (cit. on p. 13).

[23] A. Hayrapetyan et al.,
Evidence for tWZ production in proton-proton collisions at s=13 TeV in multilepton final states,
Phys. Lett. B **855** (2024) 138815, arXiv: 2312.11668 [hep-ex] (cit. on p. 13).

[24] G. Aad et al., *Search for flavor-changing neutral-current couplings between the top quark and the Z boson with proton-proton collisions at s=13 TeV with the ATLAS detector*,
Phys. Rev. D **108** (2023) 032019, arXiv: 2301.11605 [hep-ex] (cit. on p. 13).

[25] G. Aad et al.,
Observation of four-top-quark production in the multilepton final state with the ATLAS detector,
Eur. Phys. J. C **83** (2023) 496, [Erratum: Eur.Phys.J.C 84, 156 (2024)],
arXiv: 2303.15061 [hep-ex] (cit. on p. 13).

[26] *Top Quarks + X Summary Plots April 2024*, tech. rep., All figures including auxiliary figures are available at https://atlas.web.cern.ch/Atlas/GROUPS/PHYSICS/PUBNOTES/ATL-PHYS-PUB-2024-005: CERN, 2024, URL: https://cds.cern.ch/record/2896021
(cit. on p. 14).

List of Figures

List of Tables